Biochemical and Biophysical Research Communications 428 (2012) 74–79

Contents lists available at SciVerse ScienceDirect

Biochemical and Biophysical Research Communications

journal homepage: www.elsevier.com/locate/ybbrc

Deciphering complex protein interaction kinetics using Interaction Map

Danièle Altschuh [a], Hanna Björkelund [b,c], John Strandgård [b], Laurence Choulier [a], Magnus Malmqvist [b,c,d], Karl Andersson [b,c,d,*]

[a] Biotechnologie et signalisation cellulaire, Université de Strasbourg, CNRS, Irebs-ESBS, Boulevard Sébastien Brant, 67412 Illkirch, France
[b] Ridgeview Instruments AB, Ulleråkersvägen 62, 75643 Uppsala, Sweden
[c] Biomedical Radiation Sciences, Department of Radiology, Oncology and Radiation Sciences, Rudbeck Laboratory, Uppsala University, 75185 Uppsala, Sweden
[d] Ridgeview Diagnostics AB, Uppsala Science Park, 75183 Uppsala, Sweden

ARTICLE INFO

Article history:
Received 21 September 2012
Available online 9 October 2012

Keywords:
Real-time analysis
Kinetics
Heterogeneity
LigandTracer
SPR

ABSTRACT

Cellular receptor systems are expected to present complex ligand interaction patterns that cannot be evaluated assuming a simple one ligand:one receptor interaction model. We have previously evaluated heterogeneous interactions using an alternative method to regression analysis, called Interaction Map (IM). IM decomposes a time-resolved binding curve into its separate components. By replacing the reductionistic, scalar kinetic association rate constant k_a and dissociation rate constant k_d with a two-dimensional distribution of k_a and k_d, it is possible to display heterogeneous data as a map where each peak corresponds to one of the components that contribute to the cumulative binding curve. Here we challenge the Interaction Map approach by artificially generating heterogeneous data from two known interactions, on either LigandTracer or Surface Plasmon Resonance devices. We prove the ability of IM to accurately decompose these man-made heterogeneous binding curves composed of two different interactions. We conclude that the Interaction Map approach is well suited for the analysis of complex binding data and forecast that it has a potential to resolve previously uninterpretable data, in particular those generated in cell-based assays.

1. Introduction

The biophysical characterization of protein–protein interactions by use of time resolved analyses is a wide field of studies where interactions of isolated molecular components are commonly characterized using Surface Plasmon Resonance (SPR) or Quartz Crystal Microbalance (QCM) devices. Recently, novel tools for time-resolved analysis of the interaction of molecules with cells are emerging, of which LigandTracer is one. For isolated components the common basic assumption in data evaluation is that the binding curves conform to a one:one interaction. Experimental curves from cell-based assays, and also from some SPR/QCM assays, contradict the one:one binding assumption.

The fundamental problem of protein–protein interaction analysis on cells or tissue lies in the complexity of cell surfaces. A protein is likely to interact not with one form of the intended receptor at the cell-surface, but with variants of it, such as post-translationally modified receptors, activated/inactivated forms or other conformers. For example the receptor may dimerize with itself or with homologues. Interactions with completely different cell-surface-associated proteins are possible as well. One example is the EGF-EGFR interaction, which has been thoroughly analyzed and discussed during the last three decades [1–3] and which commonly results in curvilinear Scatchard plots [4]. EGFR is known to form both homodimers and heterodimers with the other members of the EGFR family (i.e. ErbB2, ErbB3, and ErbB4), and ligand-induced dimerization is necessary for activation of EGFR [5].

Each binding event may have its own set of interaction parameters. Hence it is difficult or even wrong to approximate a protein-cell interaction with reductionistic interaction models. Complex situations may also occur in the analysis of isolated components due to e.g. repeated subunits within a protein or conformational heterogeneity due to purification or surface immobilization. Current methods that are applied for the evaluation of binding curves are insufficient because they are based on regression analysis using models with limited complexity. The development of novel analysis tools, able to detect and unravel interaction complexities, is obviously required.

A method for analyzing the complexity resulting from parallel interactions in isolated molecular systems was originally developed by Svitel and co-workers [6–8]. It has been applied to probe the degree of homogeneity of the receptor population in cell-free

* Corresponding author at: Ridgeview Instruments AB, Ulleråkersvägen 62, 75643 Uppsala, Sweden. Fax: +46 18 471 3432.
E-mail addresses: daniele.altschuh@unistra.fr (D. Altschuh), hanna@ridgeview.eu (H. Björkelund), john@ridgeview.eu (J. Strandgård), laurence.choulier@unistra.fr (L. Choulier), magnus.malmqvist@bioventia.com (M. Malmqvist), karl@ridgeview.eu (K. Andersson).

0006-291X/$ - see front matter © 2012 Elsevier Inc. All rights reserved.
http://dx.doi.org/10.1016/j.bbrc.2012.10.008

protein–protein interaction analysis [6,8] to determine affinity and dissociation rates [9], and to elucidate binding mechanisms [10,11]. We have previously extended the approach to the much more complex situation of a ligand binding to living cells [3,12,13] as well as to biophysical interaction data [13].

The method of Svitel et al. [7] is well adapted for quantification of binding properties for one relatively pure component (e.g. the protein) binding to one heterogeneous component (e.g. the receptor population on the cell). The key element in this analysis lies in the use of a two dimensional distribution of interaction parameters, wherein it is assumed that each interaction of a protein in solution with a protein on a cell is monovalent. In our implementation, the distribution of interaction parameters is made discrete by creating a grid of k_a and k_d values. Each $(k_a, k_d)_{ij}$ node has a corresponding primitive interaction curve and a magnitude B_{ij}, and a heterogeneous measurement is approximated with a sum of all primitive curves scaled with the accompanying B_{ij}. Given one or more measured curves, the magnitudes of all B_{ij} can be fitted and then plotted in a surface plot as a function of k_a and k_d. We denote this plot an Interaction Map (IM) for display of interaction characteristics and heterogeneity.

While these approaches have been applied to identify binding complexity and resolve associated parameters, they have never been validated with known heterogeneous interactions systems, to the best of our knowledge. In this paper, we challenge the *Interaction Map* method by evaluating man-made heterogeneous kinetic curves generated in two ways: by injecting a protein on two co-immobilized binding partners in a Biacore Surface Plasmon Resonance (SPR) device, and by mixing two independent protein–protein interactions in a LigandTracer device.

2. Materials and methods

2.1. SPR-based protein interaction experiments

Data for the interaction of Fab57P [14] with peptides derived from the sequence of toabacco mosaic virus protein, were collected at 25 °C on a Biacore 2000® instrument (GE-Healthcare Biacore, Uppsala, Sweden) as previously described [15], except that the running buffer contained 250 mM instead of 150 mM NaCl (Hepes250:10 mM HEPES, 250 mM NaCl, 3.4 mM EDTA, 0.005% Tween 20, pH 7.4). The peptides correspond to residues 138–149 (P138–149) and 140–151 (P140–151) of the protein, with a N-terminal cysteine for surface immobilization (sequences CSYNRSSFESSSG and CNRSSFESSSGLV, respectively). Peptides were immobilized one per flow cell or two per flow cell (in 25%/75% ratios).

2.2. LigandTracer-based protein interaction experiments

105 μg trastuzumab (purified from Herceptin, Roche AB, Stockholm, Sweden) and 40 μg human serum albumin (HSA, Sigma Aldrich, St. Louis, MO) was labeled with 10 MBq ^{125}I (Perkin-Elmer, Wellesley, MA, USA) using the established Chloramine-T protocol [16]. Prior to each LigandTracer measurement, 2 μl Protein A coated magnetic beads (1.3 g/ml) (Dynabeads, Dynal A.S, Oslo, Norway), was incubated with 6 μg of the HSA binding monoclonal antibody 18080 (Abcam, Cambridge, MA, USA) in 100 μl PBS for 60 min on rotation. The magnets were washed three times with 200 μl PBS to remove excess antibody.

The interaction of ^{125}I-HSA with 18080 and/or ^{125}I-trastuzumab with Protein A was monitored in BSA pre-coated polystyrene dishes (Cat. No. 254925, Nunc, Roskilde, Denmark) using LigandTracer Grey (Ridgeview Instruments AB, Uppsala, Sweden), essentially as described previously [17]. The binding of a stepwise increase of concentration (7.8 and 24.3 nM in PBS + 1% BSA) was monitored for ^{125}I-HSA, ^{125}I-trastuzumab and a combination of ^{125}I-HSA and ^{125}I-trastuzumab (7.8 and 24.3 nM of each) during 4 h for each concentration, followed by a dissociation measurement over-night. The contribution of ^{125}I-trastuzumab and ^{125}I-HSA to the measured binding curve were altered by using ^{125}I-trastuzumab with different specific activities (numbers of radioactive nuclides per protein molecule).

2.3. Simulations

Binding curves matching the concentrations and times used for both SPR and LigandTracer experiments were simulated using the one:one interaction model for a range of different affinities and kinetics using TraceDrawer (Ridgeview Instruments AB, Uppsala, Sweden) and MATLAB 6.5 (The Mathworks Inc, MA, US).

2.4. Interaction Map generation

Under the assumption that each interaction contributing to the complex interaction can be described as a one:one interaction, the measured binding curve will be a sum of all individual one:one interactions. The measured curve can be approximated with a sum of a range of primitive binding curves, each representing a one:one interaction [3] with a unique combination of association rate k_a and dissociation rate k_d (and consequently an equilibrium dissociation constant $K_D = k_d/k_a$).

$$EstimatedCrv = \sum_{i=1}^{n}\sum_{j=1}^{m}\left[B_{ij} \times \frac{conc}{conc + k_d^i/k_a^i} \times PrimitiveCrv(conc, k_a^i, k_d^i)\right] \quad (1)$$

The constants B_{ij} represent the contribution of each primitive binding curve *PrimitiveCrv* to the estimated curve *EstimatedCrv*, and reflects the surface concentration of the corresponding receptor. There are $n \times m$ *PrimitiveCrv* with kinetic constants (k_d^i, k_a^j). Given one or more measured curves, the magnitudes of all B_{ij} were estimated by use of a non-linear fitting algorithm and were then plotted in a surface plot as a function of k_a and k_d. This plot is denoted an *Interaction Map* (IM). The surface plot may be presented in grey-scale (black = large B_{ij}, white = small B_{ij}). There are several computational issues with such an approach. Firstly, it is essential that a sufficient number of k_a and k_d values (and accompanying primitive curves) are used for representing the two-dimensional distribution of k_a and k_d, otherwise this method will have poor resolution when decomposing a measured binding curve. Secondly, it is essential to use regularization algorithms to suppress non-physical solutions to the fitting problem. Thirdly, the choice of non-linear fitting algorithm will be crucial to obtain accurate fits in reasonable time. The currently used Interaction Map method uses 24 $(k_a) \times 30$ (k_d) different nodes (with accompanying primitive curves) with kinetic parameter values evenly distributed in log-space. For interaction measurements longer than 1 h the kinetic parameter values were ($\log10(k_a) = \{2.00, 2.25, \ldots, 7.50, 7.75\}$, $\log10(k_d) = \{-6.60, -6.40, \ldots, -1.00, -0.80\}$). For interaction measurements shorter than 1 h the kinetic parameter values were ($\log10(k_a) = \{2.00, 2.25, \ldots 7.50, 7.75\}$, $\log10(k_d) = \{-5.60, -5.40, \ldots, 0.00, 0.20\}$). A Tichonov-type regularization algorithm was used, which in practice adds penalty to the sum-of-square residuals if there are many peaks in the Interaction Map. The non-linear fitting algorithm as currently implemented in Visual Basic/Visual Studio 2005 (Microsoft Inc, Mountain View, CA, USA) is stable but slow, resulting in 3–30 h computation time per map on a regular PC.

3. Results

In a first experiment, the IM method was applied to experimental SPR data. Heterogeneous data were created by injecting Fab57P

on sensor surfaces carrying different ratios of the two peptides P138–149 and P140–151, and evaluated both by regression analysis and IM. The left panel of Fig. 1 shows sets of double-referenced SPR binding curves (black curves) recorded on surfaces containing P138–149 alone (Exp. 1), 75%/25% (Exp. 2) and 25%/75% (Exp. 3) mixtures of P138–149/P140–151 and P140–151 alone (Exp. 4), together with regression analysis fits (grey curves). Data recorded on the single peptide surfaces (Exp. 1 and 4) were analyzed using the Langmuir model. In Hepes250, P138–149 binds Fab57P with a 14-fold weaker equilibrium affinity (K_D) compared to P140–151, due to a faster dissociation (Table 1). Data recorded on the mixed peptide surfaces (Exp. 2 and 3) were evaluated using the parallel reactions (PR) model. The outcome of the regression analysis depended on the input starting k_d values. The fits were good and the kinetic parameters in agreement with those obtained with the isolated peptides, when the starting k_d values were set to 10^{-4} or 10^{-3} s^{-1} (Table 1). The four data sets were also evaluated with IM (right panel). The curves representing each corresponding interaction (interaction 1: black, interaction 2: grey) are shown in the central panel. The regression analysis and IM parameters are in

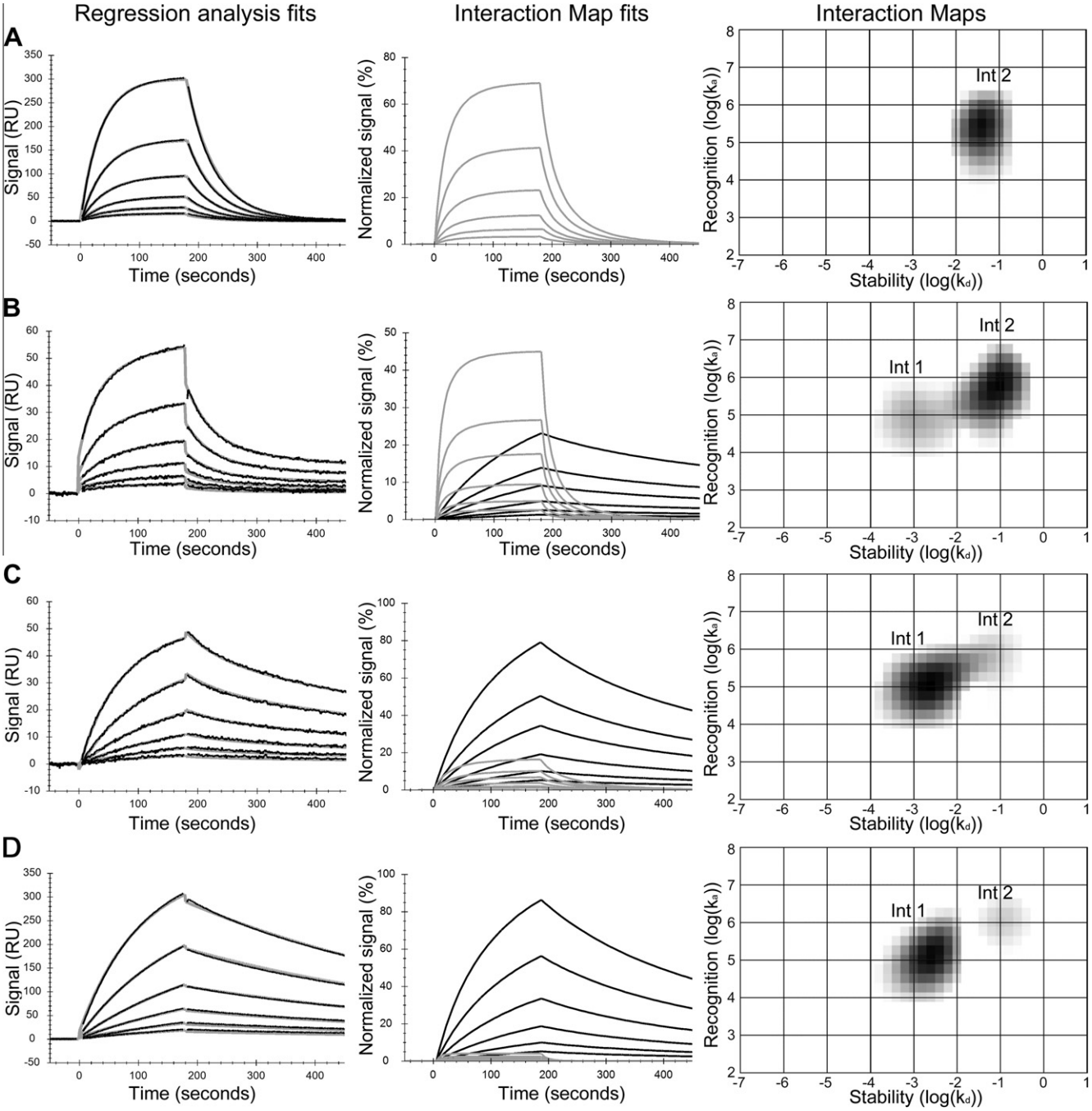

Fig. 1. Evaluation of SPR kinetic sets by regression and IM. The double-referenced binding curves correspond to the injection of six 2-fold dilution series of Fab57P samples (highest concentration 28 nM) on surfaces carrying (A) 100% P138–149 (Exp. 1) (B) 75% P138–149, 25% P140–151 (Exp. 2), (C) 25% P138–149, 75% P140–151 (Exp. 3) or (D) 100% P140–151 (Exp. 4). Between 2 and 4 buffer injections are included. The sets of kinetic curves were fitted by regression analysis using either the Langmuir model or the parallel reactions model (left column; measured curves: black, fitted curves: grey) and by IM (right column). Central column show the corresponding curves for interaction 1 (black curves) and 2 (grey curves), calculated from the peak areas in the Interaction Maps.

Table 1
Kinetic parameters for the four SPR data sets as calculated by regression analysis and IM. Since the R_{max} values in the SPR analysis is the maximum signal from the surface and the Weight in the IM calculations correspond to signal contribution under present experimental conditions, these values are not strictly comparable.

		Interaction 1				Interaction 2				
		k_{a1} (1/MS)	k_{d1} (1/s)	K_{D1} (1/M)	R_{max1} (RU) or weight (%)	k_{a2} (1/Ms)	k_{d2} (1/s)	K_{D2} (1/M)	R_{max2} (RU) or Weight (%)	Chi2
Exp. 1 100% P138–149	Regr. analysis[a]					3.2×10^5	$2.0x10^{-2}$	$6.3x10^{-8}$	966 (100%)	1
	IM					2.1×10^5	4.2×10^{-2}	2.0×10^{-7}	99%	
	Ratio RA/IM					1.5	0.5	0.3		
Exp. 2 75% P138–149 25% P140–151	Regr. analysis[b]	3.0×10^5	1.2×10^{-3}	3.9×10^{-9}	22 (26%)	5.7×10^5	2.3×10^{-2}	4.0×10^{-8}	61 (74%)	0.4
	IM	9.1×10^4	2.3×10^{-3}	2.4×10^{-8}	19%	4.4×10^5	7.1×10^{-2}	1.6×10^{-7}	70%	
	Ratio RA/IM	3.2	0.5	0.2		1.3	0.3	0.3		
Exp. 3 25% P138–149 75% P140–151	Regr. analysis[b]	3.5×10^5	1.5×10^{-3}	4.3×10^{-9}	53 (72%)	5.8×10^5	1.9×10^{-2}	3.2×10^{-8}	20 (28%)	0.2
	IM	1.1×10^5	2.0×10^{-3}	1.9×10^{-8}	83%	3.5×10^5	2.5×10^{-2}	2.5×10^{-2}	21%	
	Ratio RA/IM	3.2	0.8	0.2	1.7	0.8	0.4			
Exp. 4 100% P140–151	Regr. analysis[a]	2.9×10^5	1.8×10^{-3}	6.4×10^{-9}	430 (100%)					3.6
	IM	1.1×10^5	2.2×10^{-3}	2.0×10^{-8}	92%	1.0×10^6	1.2×10^{-1}	1.2×10^{-7}	7%	
	Ratio RA/IM	2.6	0.8	0.3						

[a] Langmuir model.
[b] Parallel reactions model, with 10^{-3} as starting values for k_{d1} and k_{d2}.

excellent agreement (Table 1), with ratios mostly <1, except for the association rate constant of the highest affinity interaction (k_{a1} ratio ~3). The proportions of the two parallel interactions, as reflected by the maximal binding capacity of the surface (R_{max}) in regression analysis and peak weight in IM, are both in accordance with the 25%/75% and 75%/25% proportions of the co-immobilized peptides.

In a second experiment, the IM method was applied to binding data measured in LigandTracer, where the ^{125}I-HSA–18080 and the ^{125}I-trastuzumab–Protein A interactions were monitored either separately (Exp. 5: Fig. 2A and Exp 8: Fig. 2E respectively) or in combination. The HSA–18080 interaction provided approximately 65% of the signal in Exp. 6 (Fig. 2B) and 47% in Exp. 7 (Fig. 2D). The two interactions displayed very similar binding properties, both maps being composed of a major (i) and a minor (ii) peak (compare Fig. 2A and E). The major peak corresponded to interactions with similar dissociation rate constants ($\log(k_d) = -5.48 \pm 0.09$), but different association rate constants: in the pure HSA–18080 measurement, Exp. 5, peak (*i*) had a higher association rate ($\log(k_a) = 4.12$) than in the pure trastuzumab–Protein A measurement, Exp. 8 ($\log(k_a) = 3.62$). In the combined measurements (Fig. 2B and C), peak (*i*) was observed somewhere in between ($\log(k_a) = 3.92$ in Exp. 6 and 3.75 in Exp. 7), reflecting the gradually shifting proportion of HSA-18080 and trastuzumab–Protein A interactions. The change in proportions was further observed in the degree of heterogeneity, where the contribution of peak (*i*) was as low as 66% in the pure HSA–18080 measurement (Exp. 5) but increased as the degree of HSA–18080 was reduced,

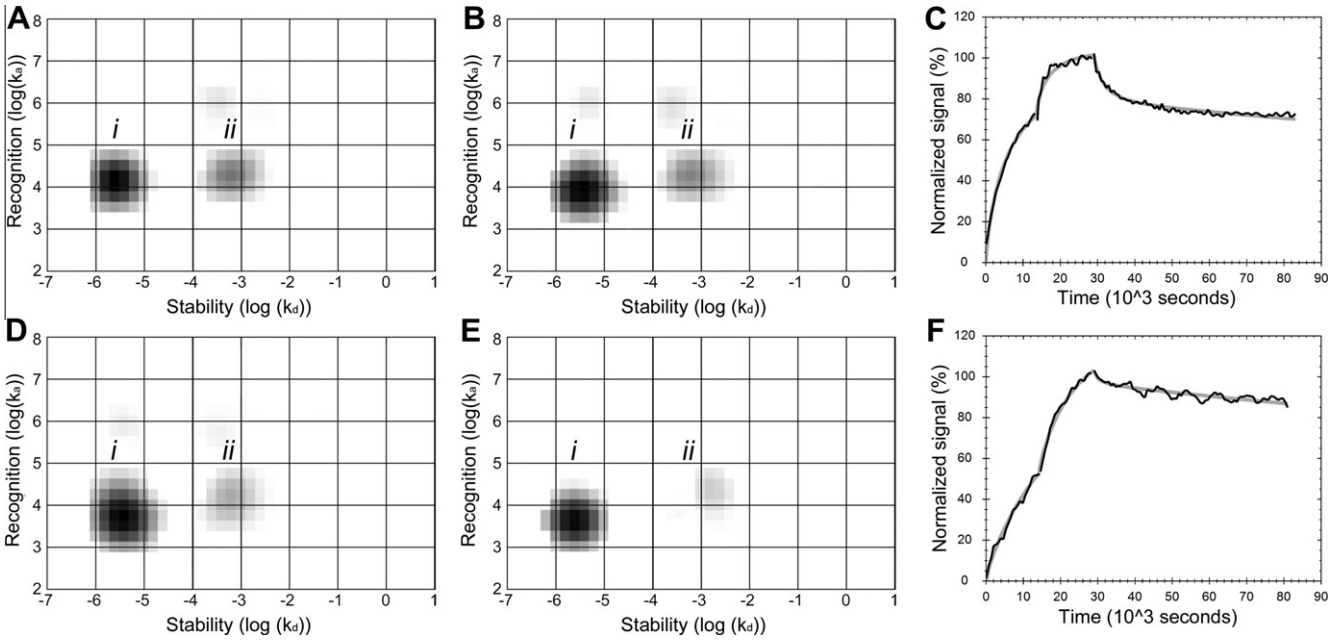

Fig. 2. Interaction Maps depicting the ^{125}I-HSA–Ab 18080 and ^{125}I-trastuzumab–Protein A interactions as measured in LigandTracer Grey. Different combinations of the HSA and the trastuzumab interactions were tested: (A) 100% HSA, 0% trastuzumab (Exp. 5), (B) 65% HSA, 35% trastuzumab (Exp. 6), (D) 47% HSA, 53% trastuzumab (Exp. 7) and (E) 0% HSA, 100% trastuzumab (Exp. 8). Corresponding LigandTracer data describing (C) Exp. 5 and (F) Exp. 8 is included. The major contributing interaction, observed as a clear peak in the map (peak *i*), had similar dissociation rate constants in all four cases ($\log(k_d) = -5.48 \pm 0.09$), but different association rate constants: $\log(k_a) = 4.12$ (Exp. 5), 3.92 (Exp. 6), 3.75 (Exp. 7), 3.62 (Exp. 8). The contribution of peak (*i*) increased when the amount of HSA was reduced, going from 66% with the pure ^{125}I-HSA–18080 interaction (Exp. 5), to 70% (Exp. 6), 80% (Exp. 7) and finally 88% for the pure ^{125}I-trastuzumab–Protein A interaction (Exp. 8). Data are representatives from duplicates or triplicates.

to 70% (Exp. 6), 80% (Exp. 7) and 88% (Exp. 8). This increase was due to the fact that peak (*ii*), located at approximately $\log(k_a) = 4$, $\log(k_d) = -3$, contributed more to the HSA–18080 interaction, compared to the trastuzumab–Protein A interaction. These experiments shows that the presence of two interactions with very similar binding properties can still be identified from subtle changes in peak patterns.

Simulated data was used to verify validity of IM for the two experimental setups. The SPR setup (6 concentrations ranging from 875 pM to 14 nM, 3 min injection) was suitable at least within the range $k_a = 10^5\ M^{-1}\ s^{-1}$ to $10^7\ M^{-1}\ s^{-1}$ and $k_d = 10^{-4}\ s^{-1}$ to $10^{-1}\ s^{-1}$, provided that the affinity $K_D = k_d/k_a < 10^{-7}$ M. For the LigandTracer setup, the two consecutive concentrations 7.8 nM and 24.3 nM (4 h each) followed by dissociation over night was suitable for analysis of interactions at least within the range $k_a = 10^3\ M^{-1}\ s^{-1}$ to $10^5\ M^{-1}\ s^{-1}$ and $k_d = 10^{-6}\ s^{-1}$ to $10^{-3}\ s^{-1}$.

4. Discussion

In this paper, we challenge the Interaction Map method with man-made complex measurements recorded with SPR or LigandTracer devices. In both experiments, different levels of heterogeneity were created: from one interaction alone, then gradually increasing the ratio of a second interaction, and finally measuring the second interaction alone. IM provided a distribution of peak weights in agreement with the ratios created for the two interactions, and peak positions in agreement with the known binding parameters of the two interactions as measured by SPR. Our data thus demonstrate that IM can decompose the cumulative binding curve of two known contributing binding partners.

Parallel interactions differing by a little more than one order of magnitude in K_D were generated by SPR using an antigen–antibody system. While classical regression analysis (parallel reactions model) of the kinetic sets produced correct results depending on the starting k_d values, IM could accurately resolve the two underlying interactions without *a priori* assumptions on either the existence or not of parallel reactions, or the range of expected kinetic parameters. In particular the weak affinity contribution in Exp. 3 (small contribution of the weak affinity interaction) was detected although the complexity of the binding curves is not visually obvious. The relative contributions of the two parallel interactions were also reasonably well evaluated (ratio of R_{max} values in regression analysis, peak weight in IM). This means that the Interaction Map method is capable of detecting complexity in an accurate manner in measurements from SPR-based instruments.

For the parallel measurements in LigandTracer, both interactions had approximately the same dissociation rate for the dominant portion of the interaction (peak *i*). This dominant portion had higher association rate in the HSA–ab18080 measurement than in the trastuzumab–protein A measurement, The HSA–ab18080 interaction also displayed a clear secondary peak (peak *ii*). When the two interactions were combined, peak *ii* gradually disappeared as the signal from the trastuzumab–protein A component was increased through modification of specific activity. This means that the Interaction Map method is capable of detecting complexity in an accurate manner without any *a priori* assumptions also in LigandTracer measurements.

Simulations were used to verify the applicability of the two experimental setups used in this paper. All interactions detected in the measurements were well within the range of interpretable affinities and kinetics for the respective experimental setups. Hence, IM has elements suitable for quantification of interaction heterogeneity for these two examples.

The original assumption for Interaction Map is that one ligand interacts with an unknown number of targets, but in the LigandTracer measurement two different molecules, each binding to a unique partner immobilized onto a magnetic bead. As long as the concentrations of the two molecules in solution (in this case HSA and trastuzumab) are the same, IM will regard them as one complex interaction. The relative signal will depend on a multitude of factors, including the specific activity (number of radioactive nuclides per molecule) of the two molecules, the number of available binding partners on the magnetic beads, and the relative affinity of the two interactions. For the purpose of illustrating the capacity of IM to accurately decipher a complex interaction, it is a valid and convenient method to use parallel independent interactions.

There are several ways to better resolve closely located peaks. One way is to increase the number of concentrations at which the interaction is quantified. Another way is to increase the number of nodes used for deriving the map and hence get a greater pixel resolution, but this increases the computational time. A third possibility is to reduce the regularization method and thereby implicitly allowing more peaks to appear. The resolution power of IM should however be compared to the expected noise and error obtained during typical kinetic analysis. Önell and Andersson [18] reported that for interaction analysis of purified molecules using Biacore instruments, the typical variation of results within a laboratory is about 15% and between laboratories up to about 50%, all when using well-behaving molecular model systems. In less well-behaving molecular systems, and in particular in cell-based assays, the typical variation is higher. The current resolution of IM is therefore adequate for the analysis of protein-cell interactions and sufficient for many cases of interaction analysis of purified proteins. More experience is required to define the limits of IM as a tool for absolute characterization of heterogeneous interactions.

This report shows that IM is an efficient way to decompose the components of biomolecular interactions of a protein to a heterogeneous member, such as cells. The approach can pin-point small differences in interaction characteristics, virtually unattainable with the current reductionistic analysis tools of real-time interaction data and completely impossible to grasp with end-point assays like immunofluorescence and RIA. IM is a complement to hypothesis driven research, where new light can be shed on complex interactions such as the EGF-EGFR interaction [3]. A drawback of the IM method is the time required to derive a map.

The potential use of IM is broad. Most importantly, it becomes possible to approach ligand-receptor interactions from a functional standpoint in order to guide and complement the assembly of theoretical interaction models [3]. There are also diagnostic applications of IM, most evidently for the benefit of cancer patients [19].

In conclusion, we have challenged the Interaction Map method for analysis of complex protein–protein interactions and proven it useful. We believe that the functional and systemic approach of IM will become an important complement to the current reductionistic analysis of heterogeneous protein interactions in both basic research and applied sciences.

Conflict of interest

HB, JS, MM and KA are employed by Ridgeview Instruments AB. MM and KA are shareholders in Ridgeview Instruments AB and Ridgeview Diagnostics AB.

Acknowledgments

D. Altschuh and L. Choulier acknowledge support from the CNRS (Centre National de la Recherche Scientifique) and UdS (University of Strasbourg).

References

[1] Y. Yarden, B.Z. Shilo, SnapShot: EGFR signaling pathway, Cell 131 (2007) 1018.

[2] F. Ozcan, P. Klein, M.A. Lemmon, I. Lax, J. Schlessinger, On the nature of low- and high-affinity EGF receptors on living cells, Proc. Natl. Acad. Sci. USA 103 (2006) 5735–5740.

[3] H. Bjorkelund, L. Gedda, P. Barta, M. Malmqvist, K. Andersson, Gefitinib induces epidermal growth factor receptor dimers which alters the interaction characteristics with (1)(2)(5)I-EGF, PLoS One 6 (2011) e24739.

[4] K. Mayawala, D.G. Vlachos, J.S. Edwards, Heterogeneities in EGF receptor density at the cell surface can lead to concave up scatchard plot of EGF binding, FEBS Lett. 579 (2005) 3043–3047.

[5] A. Citri, Y. Yarden, EGF-ERBB signalling: towards the systems level, Nat. Rev. Mol. Cell Biol. 7 (2006) 505–516.

[6] Gorshkova II, J. Svitel, F. Razjouyan, P. Schuck, Bayesian analysis of heterogeneity in the distribution of binding properties of immobilized surface sites, Langmuir 24 (2008) 11577–11586.

[7] J. Svitel, A. Balbo, R.A. Mariuzza, N.R. Gonzales, P. Schuck, Combined affinity and rate constant distributions of ligand populations from experimental surface binding kinetics and equilibria, Biophys. J. 84 (2003) 4062–4077.

[8] J. Svitel, H. Boukari, D. Van Ryk, R.C. Willson, P. Schuck, Probing the functional heterogeneity of surface binding sites by analysis of experimental binding traces and the effect of mass transport limitation, Biophys. J. 92 (2007) 1742–1758.

[9] Z. Chen, P. Earl, J. Americo, I. Damon, S.K. Smith, F. Yu, A. Sebrell, S. Emerson, G. Cohen, R.J. Eisenberg, I. Gorshkova, P. Schuck, W. Satterfield, B. Moss, R. Purcell, Characterization of chimpanzee/human monoclonal antibodies to vaccinia virus A33 glycoprotein and its variola virus homolog in vitro and in a vaccinia virus mouse protection model, J. Virol. 81 (2007) 8989–8995.

[10] H. Schmeisser, I. Gorshkova, P.H. Brown, P. Kontsek, P. Schuck, K.C. Zoon, Two interferons alpha influence each other during their interaction with the extracellular domain of human type interferon receptor subunit 2, Biochemistry 46 (2007) 14638–14649.

[11] T. Vorup-Jensen, C.V. Carman, M. Shimaoka, P. Schuck, J. Svitel, T.A. Springer, Exposure of acidic residues as a danger signal for recognition of fibrinogen and other macromolecules by integrin alphaXbeta2, Proc. Natl. Acad. Sci. USA 102 (2005) 1614–1619.

[12] P. Barta, J. Malmberg, L. Melicharova, J. Strandgard, A. Orlova, V. Tolmachev, M. Laznicek, K. Andersson, Protein interactions with HER-family receptors can have different characteristics depending on the hosting cell line, Int. J. Oncol. 40 (2012) 1677–1682.

[13] J. Nilvebrant, G. Kuku, H. Björkelund, M. Nestor, Selection and in vitro characterization of human CD44v6-binding antibody fragments, Biotechnol. Appl. Biochem. (2012). http://dx.doi.org/10.1002/bab.1033.

[14] J. Chatellier, M.H. Van Regenmortel, T. Vernet, D. Altschuh, Functional mapping of conserved residues located at the VL and VH domain interface of a Fab, J. Mol. Biol. 264 (1996) 1–6.

[15] L. Choulier, D. Laune, G. Orfanoudakis, H. Wlad, J. Janson, C. Granier, D. Altschuh, Delineation of a linear epitope by multiple peptide synthesis and phage display, J. Immunol. Methods 249 (2001) 253–264.

[16] W.M. Hunter, F.C. Greenwood, Preparation of iodine-131 labelled human growth hormone of high specific activity, Nature 194 (1962) 495–496.

[17] H. Bjorke, K. Andersson, Automated, high-resolution cellular retention and uptake studies in vitro, Appl. Radiat. Isot. 64 (2006) 901–905.

[18] A. Onell, K. Andersson, Kinetic determinations of molecular interactions using Biacore–minimum data requirements for efficient experimental design, J. Mol. Recognit. 18 (2005) 307–317.

[19] M. Malmqvist, K. Andersson, L. Lebel, H. Björkelund, L. Gedda, Method for diagnosis of individuals or animals, Patent application no. SE1200341-4, 2012.